P1.2 MICROPHYSICAL AND OPTICAL PROPERTIES OF A WAVE-CIRRUS CLOUD SAMPLED DURING THE INCA EXPERIMENT

Jean – François Gayet [(*)], Fédérique Auriol
LaMP, Université Blaise Pascal, UMR/CNRS 6016, France

Franz Immler, Otto Schrems
Alfred Wegener Institut for Polar and Marine Research (AWI), Bremerhaven, Germany

Andreas Minikin, Andreas Petzold
Institut für Physik der Atmosphäre, DLR, Oberpfaffenhofen, Germany

Joëlle Ovarlez
Laboratoire de Météorologie Dynamique, Ecole Polythechnique, Palaiseau, France

Johan Ström
Institut of Applied Environmental Research, Stockholm University, Sweden

1. INTRODUCTION

During the first field experiment in the Southern hemisphere within the international INCA project (Interhemispheric differences in cirrus properties from anthropogenic emissions) a wave-cirrus cloud was sampled by the instrumented Falcon aircraft operated by DLR and by the ground-based Lidar system operated by AWI near Punta Arenas (Chile). On the 13 April 2000, strong Westerly wind (35 m/s) over the Magallanes mountains induced a persistent wave-cirrus in the vicinity of the Punta Arenas site. The aircraft observations were co-located with the vertical profiles of the backscattering properties obtained from the Lidar system. The cirrus cloud microphysical and optical properties were inferred from the PMS FSSP-300 and 2D-C probes and the Polar Nephelometer. A quite good agreement is found between the in situ and remotely-sensed measurements in terms of water phase (water droplets or ice crystals) and extinction coefficient. Unusual high density of small non-spherical ice particles (up to 100 cm-3 with an effective diameter of 11 micrometers) inducing very large extinction coefficient (up to 15 km-1) have been evidenced.

2. INSTRUMENTATION and STRATEGY

During the INCA experiments several instruments have been mounted on the DLR Falcon aircraft for the characterization of the trace gases, aerosols and cirrus ice particles. The description of this instrumentation can be found at : www.pa.op.dlr.de/inca/. In the present study we will describe the in-situ measurements derived from the PMS FSSP-300, the PMS 2D-C and the Polar Nephelometer probes.

The PMS FSSP-300 optical particle counter basically measures particles from 0.3 to 20 μm in diameter. Because the small ice particles are not spherical (a typical asymmetry parameter of 0.77 was measured during INCA with the Polar Nephelometer, see below) the size calibration for aspherical particles proposed by Borrmann et al. (2000) was considered. Therefore the upper size limit of the FSSP-300 for cirrus measurements is actually 15.8 μm for aspherical particles. In the present study only ice particles larger than 3 μm diameter with a density of 0.9 g cm^{-3} have been considered. Coincidence effects on particle sizing have not been taken into account on data processing because these effects are hypothesized to do not significantly affect the ice crystal size spectra. Baumgardner et al. (1992) described the measurement uncertainties associated with this probe.

The PMS 2D-C probe provides information on crystal size and shape for the size range 25 – 800 μm. The method of data processing used in this study and the uncertainties on the derived microphysical parameters have already been described in detail by Gayet et al. (1996). We recall that the method provides, at 1 Hz frequency, the size spectrum distributed over 32 channels (each having a 25-μm resolution from 25 to 800 μm size range) and the usual microphysical parameters: ice particle concentration, mean particle size, and ice water content. The bulk quantities have been processed assuming empirical crystal mass-size relationship (Gayet et al., 1996). Because the sensitivity of the probe to small particles decreases with the airspeed (i.e. ~ 170 m/s with the Falcon aircraft), the six-first channels (up to 150 μm) have been corrected according to the results of Baumgardner and Korolev (1997).

The Polar Nephelometer is a unique airborne *in situ* instrument that is compatible with the PMS canister (Gayet et al., 1997). This instrument measures the scattering phase function of an ensemble of cloud particles (i. e., water droplets or ice crystals or a mixture of these particles from a few micrometers to about 800 μm diameter), which intersect a collimated laser beam near the focal point of a paraboloidal mirror. The light scattered at polar angles from ±3.49° to ±169° is reflected onto a circular array of 44 photodiodes. The laser beam is

---

Corresponding author address : LaMP, Univ. Blaise Pascal, 24 av. des Landais, 63177 Aubière, France, e-mail : gayet@opgc.univ-bpclermont.fr

provided by a high-power (1.0 W) multimode laser diode operating at λ = 804 nm. The direct measurement of the scattering phase function enables us to recognize particle types (water droplets or ice crystals), to calculate the optical parameters (extinction coefficient and asymmetry parameter, see Auriol et al., 2001). Non-absorbing ice particles randomly oriented in the sampling section are assumed in deriving bulk quantities.

A systematic comparison between the above described independent techniques and the CVI probe has confirmed the reliability of the measurements for the description of microphysical and optical cirrus properties (Gayet et al., 2002a). It should be noticed that the vertical wind component was not derived from the Falcon data due to large changes in the aircraft attitude during the flight pattern above the Lidar.

During the two INCA observation phases, a ground-based Lidar was operated by AWI. The Lidar measured the Raman and elastic backscatter coefficient profiles at λ = 532 nm and 355 nm. From these measurements the extinction coefficient profile can be derived. The depolarization and the wavelength dependence of the backscatter coefficient (β) (color index = $\ln(\beta_{532}/\beta_{355})$ / $\ln(355/532)$) give indications about the water phase (water droplet or ice crystals) and the mean particle size, respectively.

The wave-cirrus on 13 April 2000 was sampled at different levels by the Falcon aircraft with a flight pattern centered close to the AWI Lidar location. Unfortunately, during this cirrus sampling period a broken medium thin layer sometimes perturbed the remote sensing of the wave-cirrus cloud above. About 10 to 20 minutes separates the two types of measurements. Nevertheless, because of the quasi-stable dynamical and thermodynamical conditions which prevailed during that wave situation, comparisons between in situ and remote measurements may be qualitatively assessed.

3. THE WAVE-CIRRUS PROPERTIES

3.1 *In situ observations*

Figure 1.a to 1.f represent the vertical profiles of several pertinent microphysical and optical parameters obtained by the Falcon aircraft in the cloud layers between 20 :10 and 20 :35 (LT) with a flight pattern located above the AWI Lidar. Four sampling sequences were performed at distinct levels of 800, 1000, 1200 and 1300 m above the cloud base. Obviously, the cloud parameter values must be considered only as estimates because of the natural cloud inhomogeneities, the cloud time-variability and the different geographical locations of the aircraft during the corresponding flight sequences. Nevertheless, these vertical profiles obtained during the 25 minutes duration are rather well correlated with the Lidar profiles as we will discuss in § 3.2. The results on Figs. 1 clearly reveals two distinct and decoupled cloud layers. The lower layer observed between 6900 m/-29°C and 7200m/-32°C is a supercooled water cloud because the values of the asymmetry parameter derived from

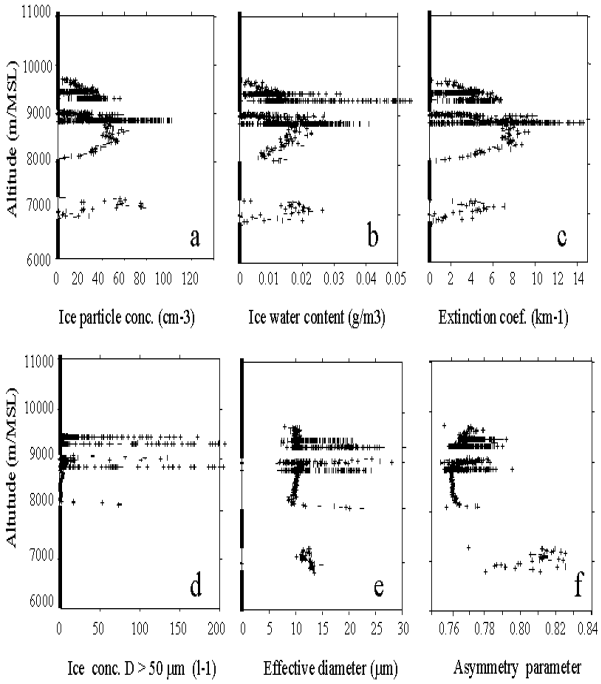

Figure 1 : *Vertical profiles of the following parameters : (a) ice particle concentration, (b) ice water content, (c) extinction coefficient, (d) ice density of particles (D> 50 μm), (e) effective diameter and (f) asymmetry parameter.*

the Polar Nephelometer measurements (Fig. 1.f) are ranged between 0.80 and 0.823 (see for instance Raga and Jonas, 1993). The upper layer is detected from 8000 m/-38°C to 9500 m/-49°C with a gap of 200 m in the profile measurements near 9000 m. From the microphysical and remotely-sensed properties (see below), the cloud was identified as a wave-cirrus. The values of the asymmetry parameter are lower than 0.79 which is a typical signature of non-spherical ice particles (Gayet et al., 2002b). The profile in Fig. 1.a show that the ice particle concentration increases from the cloud base to the mid-layer to about 60 cm-3 whith large horizontal heterogeneities and maximum values up to 110 cm-3. The mean effective diameter (Fig. 1.e) is about 11 μm with fluctations up to 25 μm at the four distinct sampling levels. The ice water content profile (Fig. 1.b) also reveals large fluctuations (mean and maximum values of 20 mg/m3 and 55 mg/m3 respectively) and a similar profile is observed with the extinction coefficient (Fig. 1.c) where values up to 15 km-1 are reported. The concentration of large ice particles (D> 50 μm) reveals peaks up to 250 l-1(Fig. 1.d) and subsequent fluctuations of the asymmetry parameter (Fig. 1.f) are also noticed (0.76 to 0.79).

In order to illustrate the cloud horizontal heterogeneities, we have reported on Fig. 2 time-series of the parameters above presented with the relative humidity (with respect to the ice, see Ovarlez et al., 2002). All these parameters have been obtained by the Falcon during a 4-min sample of the cloud at the 8800 m/-43°C level. The results show that during this flight sequence, the aircraft

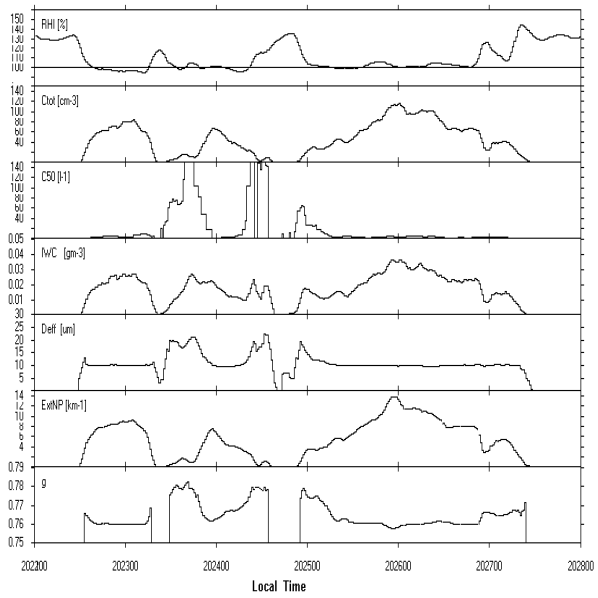

Figure 2 : *Time-series of the parameters measured by the Falcon at 8800 m/-43°C in the wave-cirrus cloud. RHI : Relative humididy (with respect to ice, Ovarlez et al., 2002), Ctot : ice particle concentration, C50 : concentration of particles (D>50 mm), IWC : ice water content, ExtNP : extinction coefficient, g : asymmetry parameter.*

sampled three distinct cirrus cloud patches which have rather similar properties. High concentration (larger than 80 cm-3) of small ice particles with a constant effective diameter (Deff = 11 μm) are observed within the main part of the cirrus cloud. Subsequently, the asymmetry parameter has a quasi-constant value (0.760) and the concentration of particle larger than 50 μm is very low (a few particles per liter). It should be noticed that the occurrence of the numerous small ice crystals cannot be due to the shattering of large ice crystals on the probe inlets because only a few particles (larger than 50 μm) were detected by the 2D-C probe in these regions (Gayet et al., 2002).

Fig. 3 illustrates a typical example of results observed near the middle part of the cirrus cloud (at 20:26, see Fig. 2). The left-panel display the FSSP-300 and 2D-C particle size distribution with the subsequent values of the pertinent parameters whereas the right-panel represents the measured (Polar Nephelometer) and the theoretical scattering phase functions, the latest being calculated from the FSSP-300 size distribution assuming spherical particles. The comparison of these two phase functions shows that scattering by ice particles is considerably stronger at the side angles between 80 and 120°, leading to a significantly smaller g-value (0.758) than for the scattering by spherical particles.

Coming back on the time-series on Fig. 2, a noteworthy observation concerns the relationship between the cloud properties and the humidity measurements. As a matter of fact, outside the cloud the humidity reveals supersaturations (with respect to ice) of about 130%, whereas the humidity drops to the water vapor equilibrium

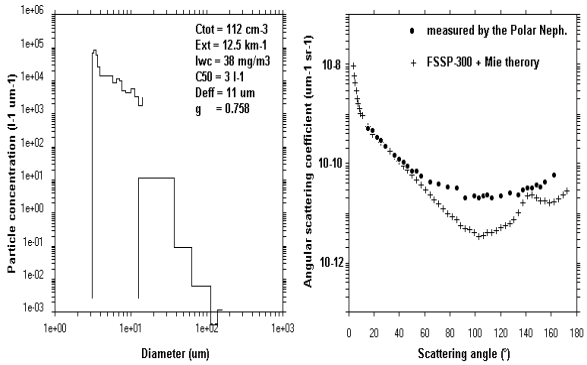

Figure 3 : *Example of in-situ measurements obtained at 20 :26 (LT). Left panel : FSSP-300 and 2D-C size distributions and values of the corresponding pertinent parameters. Right panel : Measured (Polar Nephelometer) and theoretical scattering phase functions, the latter being calculated from the FSSP-300 measurements and assuming ice spheres.*

(100%) within the main cloud part where only small ice particles are observed. This means that all the available water vapor was fully consumed by the formation of the numerous ice crystals offsetting the growth of these ones. Larger ice crystals are detected (C50) only on the fringes of the cloud where the water vapor was still available for a further growth. This feature explains the large gradients in the effective diameter and asymmetry parameter in Figs. 1.

3.2 *Remote-sensing observations*

Despite non-synchroneous observations, comparisons between in situ and remote measurements may be qualitatively assessed because of the quasi-stable dynamical and thermodynamical conditions which prevailed during that wave situation.

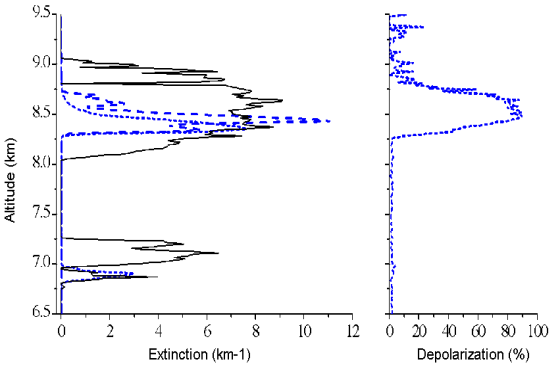

Figure 4 : *Vertical profiles of the extinction coefficient (blue lines) and volume depolarization (at 532 nm) measured by the AWI Lidar at 20 :25 LT (dotted) and 20 :33 LT (dashed). It is superimposed by the extinction profile derived from the Polar Nephelometer (solid line) when the Falcon was nearby the Lidar (± 20 km) at about the same time (± 15 mn).*

Fig. 4 displays the extinction profile and volume depolarization at 532 nm derived from the AWI Lidar measurements performed at 20:25 and 20:33 (LT). The profile of the extinction coefficient from the Polar Nephelometer has been super-imposed on the Figure by considering only measurements where the Falcon was nearby the Lidar. Despite non-synchronized data a qualitative good agreement is observed between the two measurements. Considering the lower cloud layer, a zero–value of the depolarization is due to water droplets and confirms the in situ observations (Fig. 1.f). On the contrary in the cirrus cloud above strong depolarization indicates the presence of non-spherical ice crystals. Furthermore, the interpretation of the Lidar measurements confirms the very high value of the extinction coefficient (up to 12 km-1). The color index which is actually around zero in cirrus clouds is significantly increased to about 0.8 in the wave-cirrus. According to the scattering theory (Liu et al., 2001) this indicates the presence of very small particles. This is again in a qualitative agreement with the in situ observations.

4. CONCLUSIONS

The results show that the wave-cirrus cloud exhibits a rather large number density of small ice crystals (up to 100 cm-3 with an effective diameter of 11 micrometers). The occurrence of these small ice crystals cannot be due to the shattering of large ice crystals on the probe inlets because no large particles were detected by the 2D-C probe. These characteristics lead to an unusual large extinction coefficient (up to 12 km-1) which is confirmed from both the Polar Nephelometer measurements and the Lidar retrievals. Because an asymmetry parameter of about 0.77 was measured by the Polar Nephelometer, the small ice particles are not spherical. Humidity measurements reveal that all the available water vapor (supersaturation excess with respect to ice) was fully consumed by the formation of the numerous ice crystals offsetting the growth of these ones. Larger ice crystals were detected (2D-C probe) only on the fringes of the cloud where the water vapor was still available for a further growth. This feature leads to large gradients in the asymmetry factor and effective diameter. The Lidar measurements revealed the decoupled-layer feature of the wave-cirrus sampled cloud. Because no water droplets have been detected near the wave-cirrus cloud base this suggests the occurrence of homogeneous freezing of solution droplets at this cloud formation level. On the contrary, the lower cloud was identified by the two instruments as a supercooled water droplet layer.

Acknowledgements. This work was funded by European Union contract EVK2-CT-1999-00039. Thanks are due to our colleagues for their helpful contribution to the experiments. This work is also supported by the INSU/PATOM. We are very grateful to the members of the DLR who operated the Falcon aircraft during the two experiments. We acknowledge all the people that supported us at the Punta Arenas and Prestwick airports both before and during the campaigns.

5. REFERENCES

Auriol F., J-F Gayet, G. Febvre, O. Jourdan, L. Labonnotte and G. Brogniez, 2001 : In situ observations of cirrus cloud scattering phase function with 22° and 46° halos : Cloud field study on 19 February 1998. *J. Atmos. Sci.,* 58,3376-3390.

Baumgardner, D., J.E. Dye, R.G. Knollenberg, and B.W. Gandrud,1992: Interpretation of measurements made by the FSSP-300X during the Airborne Arctic Stratospheric Expedition, *J. Geophys. Res.*, 97, 8035-8046.

Baumgardner D. and A. Korolev, 1997 : Airspeed corrections for optical array probe sample volumes. *J. Atmos. Ocean. Tech*., 14, 1224-1229.

Borrmann S., Luo B. and Mishchenko M., 2000 : Application of the T-Matrix method to the measurement of aspherical (ellipsoidal) particles with Forward Scattering Optical counters. *J. Aerosol Sci.* (31)7, 789-799.

Gayet, J-F, G. Febvre, G. Brogniez, H. Chepfer, W. Renger and P. Wendling, 1996 : Microphysical and optical properties of cirrus and contrails : Cloud field study on 13 October 1989. *J. Atmos. Sci*., 53, 126-138.

Gayet, J-F, O. Crépel, J-F Fournol and S. Oshchepkov, 1997 : A new airborne Polar Nephelometer for the measurements of optical and microphysical cloud properties. Part I: Theoretical design. *Annales Geophysicae*, 15, 451-459.

Gayet J-F, F. Auriol, A. Minikin, J. Ström, M. Seifert, Radovan Krejci, A. Petzold, G. Febvre and U. Schumann, 2002a : Quantitative measurement of the microphysical and optical properties of cirrus clouds with four different in situ probes : Evidence of small ice crystals. Submitted to *Geophys. Res. Lett.*.

Gayet J-F, S. Asano, A. Yamazaki, A. Uchiyama, A. Sinyuk , O. Jourdan and F. Auriol, 2002b : Two case studies of continental-type water and maritime mixed-phased stratocumuli over the sea. Part I : Microphysical and Optical properties. *J. Geophys. Res.*, in print.

Ovarlez J, F. Auriol, J-B Brissot, R. Busen, J-F Gayet, K. Gierens, H. Ovarlez, U . Schumann and J. Ström, 2002 : Water vapour measurements inside cirrus clouds in Northern and Southeren hemispheres during INCA. Submitted to *Geophys. Res. Lett.*.

Raga, G.B. and P. R. Jonas, 1993 : Microphysical & radiative properties of small cumulus clouds over the sea. *Q.J.R. Meteor. Soc.*, 119, 1399-1417.

Liu L., M.I. Mishchenko, Constraints on PSC particle microphysics derived from lidar observations*, J. of Quant. Spec. Radiat. Trans.*, 70, 817-831, 2001.